engineering proceedings

MDPI

Proceeding Paper

A New Approach to the Application of SMA Strain Sensors for Structural Health Monitoring of COPVs †

Alexander Hiekel *, Björn Senf and Welf-Guntram Drossel

Fraunhofer Institute for Machine Tools and Forming Technology, 09126 Chemnitz, Germany; bjoern.senf@iwu.fraunhofer.de (B.S.); welf-guntram.drossel@iwu.fraunhofer.de (W.-G.D.)

* Correspondence: alexander.hiekel@iwu.fraunhofer.de; Tel.: +49-351-4772-2068

† Presented at the 15th EASN International Conference, Madrid, Spain, 14–17 October 2025.

Abstract

Type-IV composite overwrapped pressure vessels (COPVs) enable efficient hydrogen storage but experience severe thermal and mechanical loads that threaten structural integrity, necessitating reliable condition monitoring. This work investigates pseudo-elastic shape-memory alloy (SMA) strain gauges as a cost-effective alternative to fiber-optic systems for monitoring COPVs. Their performance was characterized on composite specimens using four-point bending tests. Additionally, a finite element model analyzed surface-strain behavior as a function of COPV geometry parameters and ambient temperature, enabling identification of optimal quarter-bridge measurement configurations.

Keywords: shape-memory alloys; strain sensors; composite overwrapped pressure vessels; structural health monitoring

1. Introduction

Type-IV composite overwrapped pressure vessels (COPV) provide one of the most efficient methods to store hydrogen as an alternative energy source to fossil fuels. Due to the lower weight, higher specific strength and increased fatigue resistance compared to conventional metallic pressure tanks, the fields of application range from energy, transportation and aerospace to the defense sector [1]. In these operating scenarios, extreme temperature fluctuations and critical loads have a decisive effect on the integrity of the tank structure. Monitoring the condition of the COPV is, therefore, essential to ensure safe operation and predict service life. Condition monitoring systems using piezoresistive, piezoelectric or fiber-optic strain sensors have already been the subject of numerous past and current investigations [2–4]. Although the latter offer a high data transmission rate as well as low susceptibility to interference and influence on the mechanical performance of the tank, these advantages are offset by high acquisition costs and complex installation work [5]. In contrast, conventional strain gauge elements are considerably more cost-efficient, but are unsuitable for use in COPVs due to the low maximum cyclical strain of approx. 0.2%.

An alternative approach is offered by pseudo-elastic shape-memory alloys. These can achieve reversible strains of up to 8%, which results from a phase transformation of the material under mechanical load [6]. Since the phase transformation correlates with a strong change in electrical resistance, strain gauge elements can be realized with a higher elastic-deformation capability, fatigue strength and a higher strain factor than conventional CuMnNi-based ones [7]. This paper characterizes the applicability of these shape-memory-based strain gauges for condition monitoring of COPVs. On the one hand, the focus lies

Check for updates

Academic Editors: Spiros Pantelakis, Andreas Strohmayer and Gustavo Alonso

Published: 27 April 2026

Copyright: © 2026 by the authors. Licensee MDPI, Basel, Switzerland. This article is an open access article distributed under the terms and conditions of the Creative Commons Attribution (CC BY) license.

on the characterization of the shape-memory alloy (SMA) strain sensor on the composite material. For this purpose, SMA strain sensors were applied to test specimens of the tank material, and the sensor response was characterized in four-point bending tests to obtain the characteristic curve. A second focus is the selection of a suitable measuring arrangement. In contrast to conventional steel tanks, COPVs consist of several layers of wound carbon-fiber-reinforced composites with directional-dependent material properties. This anisotropy influences the direction of the measurable strains on the tank surface. For the evaluation, a finite element model of the COPV was developed and the strains on the surface were analyzed as a function of the temperature and sensor orientation in a parameter study. Based on the results, suitable arrangements of quarter-bridge circuits were identified with the aim of achieving a high signal strength regarding the mechanically induced strain and a high level of compensation for temperature-related influences.

2. Materials and Methods

2.1. SMA Strain Sensor

Pseudo-elasticity in SMAs arises from a reversible, stress-induced phase transformation between the high-temperature austenite phase and the martensitic phase [8]. When mechanical loading is applied above the austenite finish temperature, the material undergoes a transformation from austenite to detwinned martensite, allowing large recoverable strains without permanent deformation. Upon unloading, the reverse transformation restores the original lattice structure, enabling strain recoveries of several percent—significantly higher than those achievable in conventional metals. Shape-memory alloy sensors exploit this pseudo-elastic effect by correlating the phase transformation with pronounced changes in electrical resistance. As the material transitions between phases under mechanical load, the associated microstructural rearrangements result in a distinct, measurable resistance variation. This enables SMA elements to function as strain sensors with high elastic-deformation capability, excellent fatigue resistance, and substantially higher gauge factors compared to conventional strain gauges based on constantan, as shown in Table 1 [7]. These properties make SMA-based sensors particularly well-suited for monitoring structures exposed to large cyclic or multi-axial deformations.

Table 1. Comparison of characteristic parameters strain sensors based on SMA and constantan.

Sensor Material	SMA	Constantan
Gauge factor	3–8	2
Temperature range	−40 °C to 120 °C	−70 °C to 200 °C
Fatigue resistance	10^6 cycles at 0.8% 10^7 cycles at 0.5%	10^6 cycles at 0.23%

For the characterization of the mechanical and thermal behavior, SMA wire specimens with a diameter of 50 µm were experimentally investigated. In the first test, a uniaxial tensile experiment was performed to measure the change in electrical resistance of a 100 mm-long wire under a constant applied strain at room temperature. In a second experiment, the electrical resistance was recorded as a function of temperature to quantify the thermal sensitivity of the material. Together, these measurements provide the basis for evaluating the suitability of the SMA wires for strain-monitoring applications.

2.2. Application of SMA Strain Sensors on COPV Test Samples

For the experimental characterization, the SMA strain sensors were applied as wires onto rectangular test specimens made from the COPV material as shown in Figure 1a. These specimens consisted of consolidated towpreg laminates, where towpreg refers to

continuous carbon-fiber tows pre-impregnated with a thermoset resin system. Towpregs enable precise fiber alignment, controlled resin content, and reproducible mechanical properties, making them representative of the filament-wound composite layers used in Type-IV pressure vessels. Because SMA wires are difficult to solder due to their alloy composition and oxide layer formation, electrical connections were established using crimp barrels, which provide a reliable, low-resistance mechanical bond to the measurement leads. The surface of the carbon-fiber-reinforced towpreg material is electrically conductive; therefore, a thin glass-fiber insulation layer was applied beneath the SMA wires to prevent short circuits and ensure a well-defined current path through the sensor element.

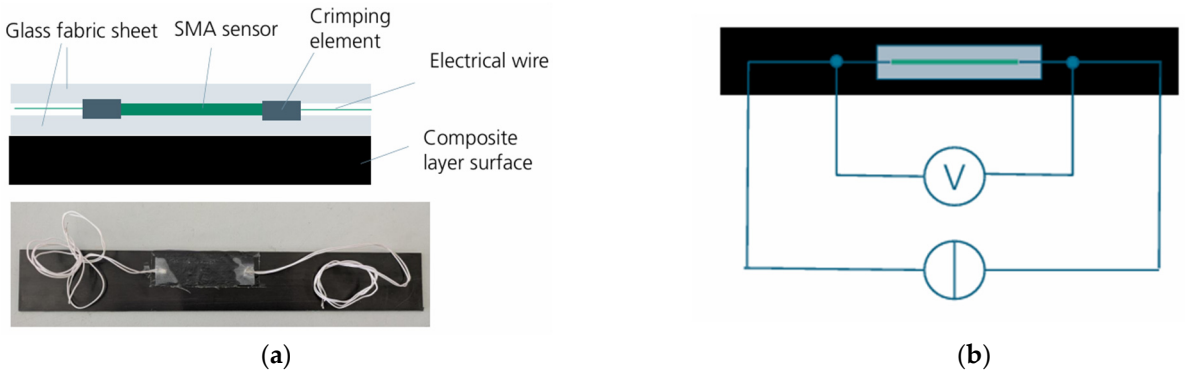
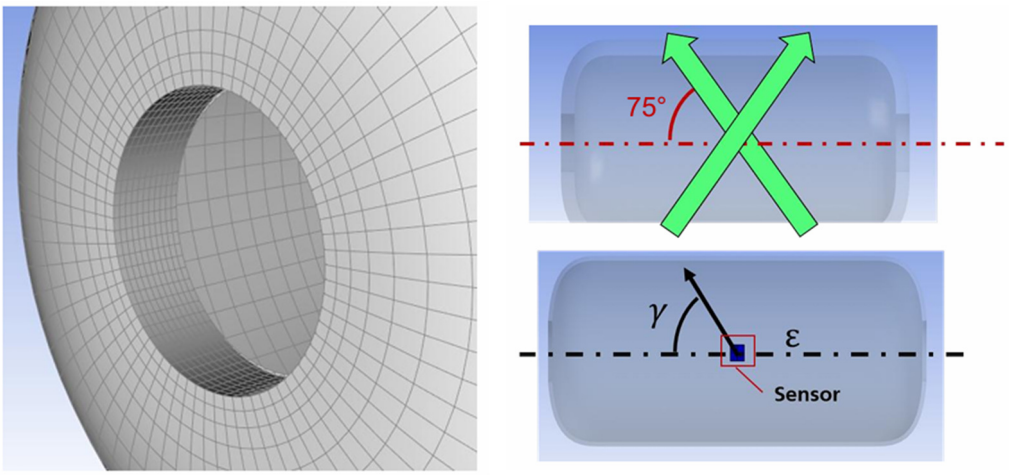


Figure 1. (**a**) Application of SMA strain sensors on towpreg test samples and (**b**) circuit diagram of the 4-wire measurement for measuring the change in resistance of the SMA strain sensor.

Resistance changes in the SMA wires were measured using a four-wire measurement technique as shown in Figure 1b. This method separates the current- and voltage-sensing leads, thereby eliminating the influence of contact and lead resistances. As a result, it enables highly accurate detection of small resistance variations, improves measurement stability under mechanical loading, and is particularly suitable for materials such as SMAs, where precise resistance tracking is essential for strain monitoring. The sensor response was evaluated using a four-point bending test, in which the specimen is supported at two outer points while the load is applied at two inner points, generating a constant bending moment in the central region. This setup ensures a well-defined and uniform strain distribution along the gauge section of the SMA wire, avoiding localized stress peaks that may occur in three-point bending. The four-point bending method offers high reproducibility, improved control over the applied strain, and reduced sensitivity to shear effects, making it particularly suitable for accurately correlating mechanical deformation with the electrical resistance changes in the SMA strain sensors.

2.3. Simulation Model for the Identification of Optimal Sensor Orientation on the COPV Surface

The simulation model was created using the ACP tool in ANSYS Mechanical 2024 R2, as shown in Figure 2a. A simplified representation of the COPV structure was chosen to assess the general applicability and robustness of the modeling approach. The material parameters were taken from the ANSYS material database and are listed in Table 2, which highlights the directional dependence of the composite properties, particularly the Young's modulus as a mechanical parameter and the coefficient of thermal expansion as a thermal-influence factor. The liner was modeled as the inner reference surface, onto which ten composite layers were applied. These layers were defined with alternating winding angles of $\pm 75^{\circ}$ with respect to the longitudinal axis of the cylindrical tank, reflecting the characteristic filament-wound architecture of the planned COPV.



(**a**) (**b**)

Figure 2. (**a**) Finite element model of the COPV with 10 layers and (**b**) orientation of the COPV layers and the sensor on the COPV surface.

Table 2. Material parameters of the COPV layer material used in the simulation.

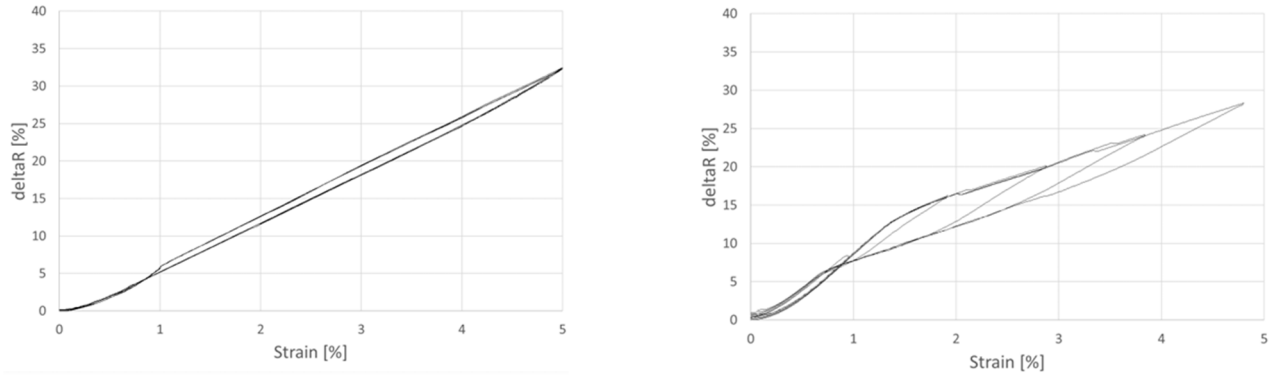
Direction	Modus of Elasticity [MPa]	Coefficient of Thermal Expansion [°C]
Normal to fiber	121,000	-4.7×10^{-7}
Orthogonal to fiber	8600	3.5×10^{-5}

For the evaluation of the sensor response, an eleventh layer was introduced as a dedicated sensor layer. This layer was modeled as a linear-elastic material without thermal influences and assigned a Young's modulus that is reduced by a factor of 1000 compared to the ten structural composite layers of the tank. The sensor layer was bonded to the tank surface using a fully coupled contact definition, ensuring that it experiences the full surface-strain field while exerting no mechanical influence on the structural behavior of the vessel. This approach enables efficient extraction of strain values at arbitrary points and along any chosen orientation relative to the longitudinal axis of the tank.

3. Results

3.1. Results of the Experimental SMA Strain-Sensor Characterization

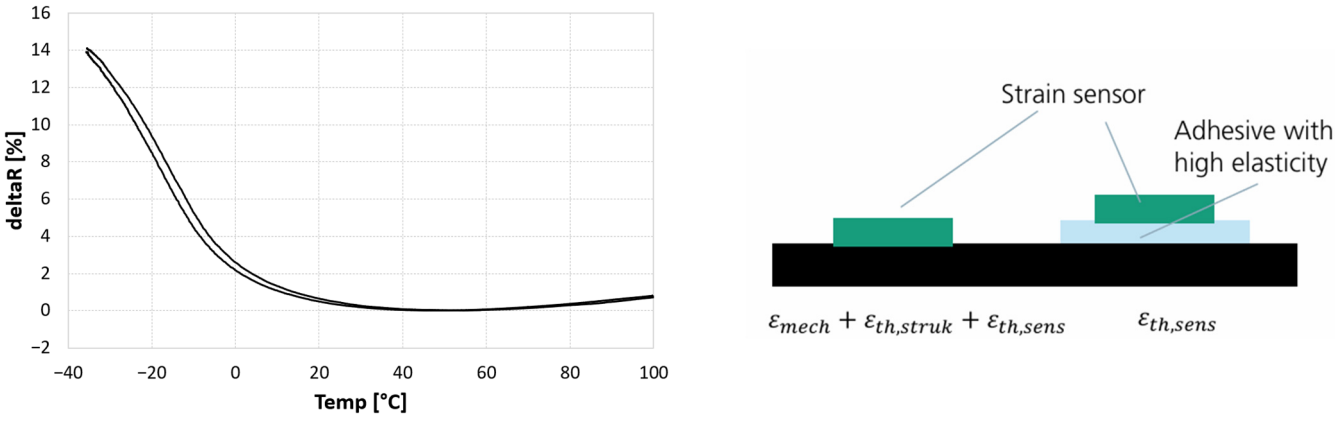
The diagrams in Figure 3 illustrate the change in electrical resistance of the SMA wire specimens as a function of the applied mechanical strain. All wire samples had a diameter of 50 µm but were sourced from two different manufacturers (Fort Wayne Metals and SAES Getters). The Fort Wayne Metals wire exhibits a noticeably lower mechanical hysteresis than the SAES Getters wire, with almost no hysteresis visible up to approximately 0.9% strain. At higher strain levels, stress-induced martensite formation occurs, and the forward and reverse transformation between martensite and austenite introduces a characteristic hysteresis. For sensor applications, the strain range up to 1% is of particular interest, as SMA wires in this regime can achieve cyclic lifetimes of several million load cycles while maintaining stable sensor characteristics.



(**a**) (**b**)

Figure 3. Change in the electrical resistance of SMA wires with a diameter of 50 µm depending on mechanical strain: (**a**) Fort Wayne Metals and (**b**) SAES Getters.

The results of the thermal characterization shown in Figure 4 indicate that the electrical resistance varies by approximately 1% around room temperature to 100 °C but increases sharply at temperatures below about 5 °C. This behavior implies a R-phase transformation [9] within the material. Such material-specific effects constitute a disturbance factor in sensor design, where the minimal temperature dependence of the sensing element is desired. One possible compensation strategy is to apply two sensors to the target surface: one sensor is directly bonded to the surface and, therefore, experiences both mechanical strain and thermal effects, while the second sensor is mechanically decoupled from the substrate by a highly elastic carrier layer, causing it to respond only to thermal influences, as described by the curve in Figure 3. The measured temperature response of the reference sensor can then be used to compensate for the temperature-induced contribution in the strain-sensor signal.

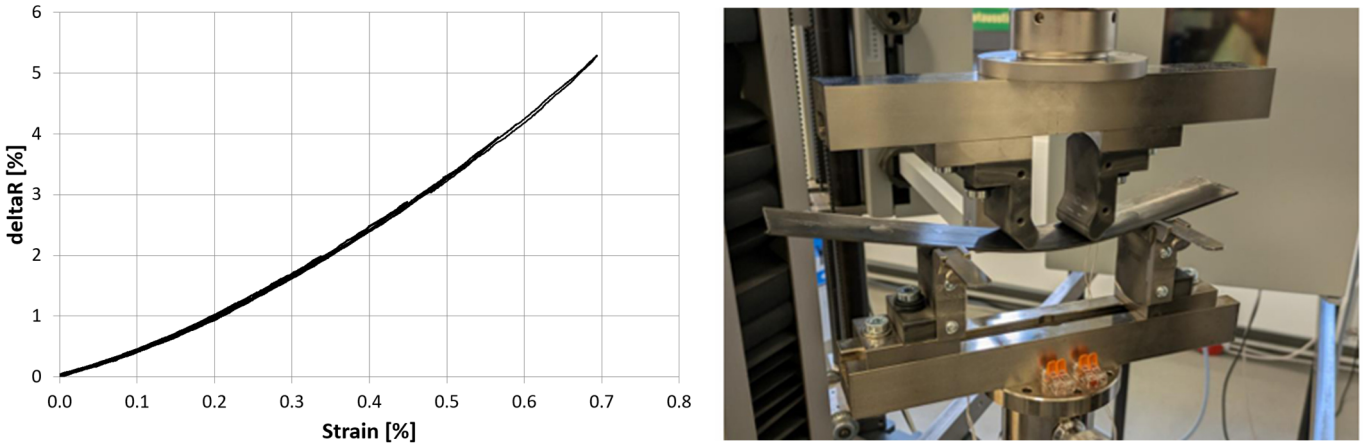


(**a**) (**b**)

Figure 4. (**a**) Change in the electrical resistance of the Forty Wayne Metals SMA wire (Ø 50 µm) depending on the ambient temperature. (**b**) Method for the compensation of temperature effects.

Figure 5 presents the results of the four-point bending tests. The towpreg specimen with the applied SMA sensing layer was cyclically loaded and unloaded in four stages up to strain levels of 0.34%, 0.45%, 0.56%, and 0.69%. The corresponding curves show almost perfect overlap, indicating the absence of degradation effects throughout the testing sequence. The sensor integration remained intact, with no detachment or damage observed. The measured resistance response accurately reflects the strain behavior of the SMA wire. The chosen methodology—including the mechanical contact configuration and the four-wire measurement technique—proved well-suited for capturing resistance changes. In

particular, the strain range between 0.3% and 0.7% exhibits a nearly linear relationship between strain and resistance change, with no observable hysteresis.



(**a**) (**b**)

Figure 5. (**a**) Change in the electrical resistance of the Forty Wayne Metals SMA wire (Ø 50 µm) on the towpreg test sample depending on the ambient temperature. (**b**) Experimental setup of the four-point bending test.

3.2. Simulation Results

Figure 6 presents the results of the finite element simulation. In the model, the tank was constrained only at one end, allowing free axial expansion. A constant internal pressure of 2 MPa was applied, and the temperature was varied between −50 °C and 150 °C. The diagram illustrates the strain response of the sensor layer for different orientation angles relative to the longitudinal axis of the tank.

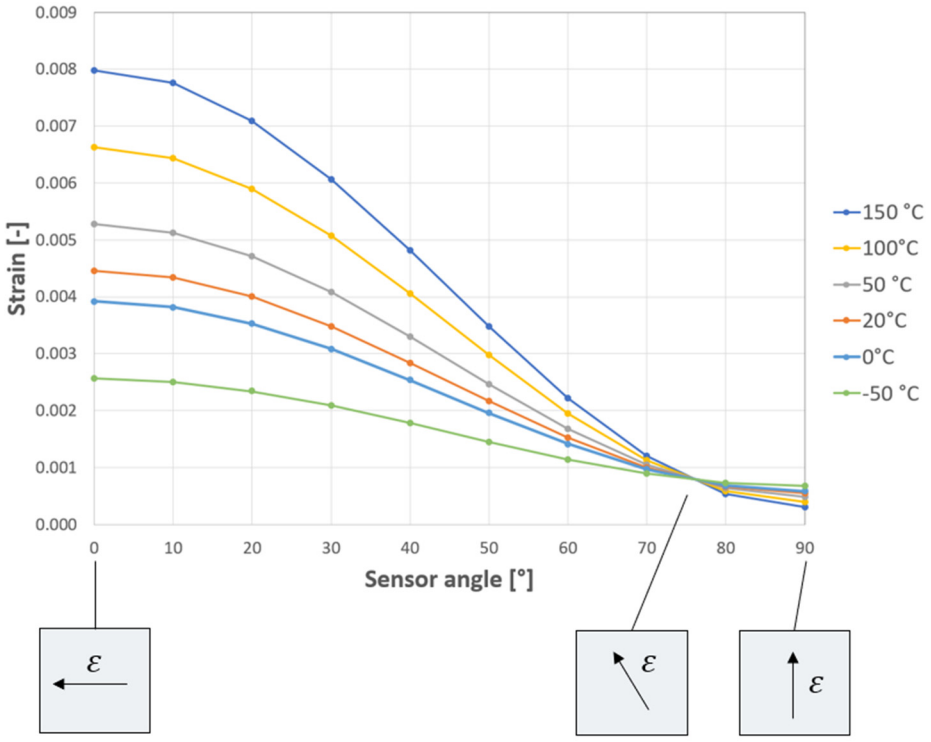


Figure 6. Strain amplitude as a function of sensor angle relative to the longitudinal axis of the COPV model at different ambient temperatures.

Sensors oriented parallel to the longitudinal axis exhibit the highest strain signals under internal pressure, but they are also strongly affected by temperature changes. In contrast, sensors aligned in the circumferential direction show lower mechanical strain amplitudes yet significantly reduced thermal sensitivity. Owing to the symmetry of the composite layup, there exists an intermediate orientation in which the effective thermal expansion is close to zero. This direction is located near the winding angle of the $\pm 75^{\circ}$ fiber layers and represents a promising alignment for minimizing thermal disturbances in strain measurements. The absolute strain values in the longitudinal direction are larger than those in the circumferential direction. This can be attributed to the fact that, due to the high winding angle, the effective Young's modulus along the tank axis is relatively low, as the material response is dominated by properties transverse to the fiber direction, which are significantly lower than those along the fibers, as shown previously in Table 2. Additionally, an equal number of layers was assumed for all regions of the tank. In real COPVs, however, the dome sections are reinforced with additional windings, resulting in higher circumferential stiffness and, consequently, larger circumferential strains under internal pressure. This reinforcement must be incorporated into future refinements of the simulation model to achieve a more realistic strain distribution.

4. Discussion

This work presented the characterization and evaluation of pseudo-elastic shape-memory alloy (SMA) strain sensors for condition monitoring of Type-IV composite over-wrapped pressure vessels. The mechanical and thermal behavior of SMA wires was analyzed, demonstrating a stable and nearly hysteresis-free response in the strain range up to 1%, which is particularly suitable for long-term cyclic loading. Sensor integration on towpreg specimens was successfully achieved using crimped electrical contacts, glass-fiber insulation, and a four-wire measurement technique, enabling precise detection of resistance changes. Four-point bending tests confirmed the robustness of the sensor arrangement and revealed a linear correlation between strain and resistance change within the operational strain range. A finite element model of the COPV was developed, showing how strain magnitudes and thermal influences depend strongly on sensor orientation relative to the winding angle of the composite layers.

Future work will refine the simulation by incorporating realistic dome reinforcement and variable layer counts to better represent the actual strain distribution in COPVs. Additionally, dual-sensor concepts will be implemented to compensate temperature-induced effects more effectively. Further experimental investigations are planned on tubular towpreg specimens, onto which SMA sensors will be applied. These specimens will be tested under internal pressure and controlled temperature conditions in a climate chamber to validate the simulation results and optimize the modeling approach based on experimental data. Ultimately, the integration of SMA-based strain sensors directly onto COPV surfaces represents a promising and cost-efficient strategy for structural health monitoring, enabling improved lifetime prediction and enhanced operational safety of hydrogen storage systems.

Author Contributions: Conceptualization, A.H. and B.S.; methodology, A.H. and B.S.; software, A.H.; validation, A.H. and B.S.; formal analysis, A.H.; investigation, A.H.; resources, W.-G.D.; data curation, A.H.; writing—original draft preparation, A.H.; writing—review and editing, B.S. and W.-G.D.; visualization, A.H. and B.S.; supervision, B.S. and W.-G.D.; project administration, B.S.; and funding acquisition, B.S. and W.-G.D. All authors have read and agreed to the published version of the manuscript.

Funding: This research was funded by the Saxon State Ministry of Science, Culture and Tourism (SMWK) and the Sächsische Aufbaubank, grant references 100688193 and 100686714.

Institutional Review Board Statement: Not applicable.

Informed Consent Statement: Not applicable.

Data Availability Statement: Raw and processed data required to reproduce these findings cannot be shared at this time as the data also form part of an ongoing study. Data sharing is not applicable in this article.

Acknowledgments: The authors would like to thank their funding agencies as well as the M-era. Net consortium.

Conflicts of Interest: The authors declare no conflicts of interest. The funders had no role in the design of the study; in the collection, analyses, or interpretation of data; in the writing of the manuscript; or in the decision to publish the results.

Abbreviations

The following abbreviations are used in this manuscript:

COPV	Composite Overwrapped Pressure Vessel
SMA	Shape-memory Alloy

References

1. Bouhala, L.; Polesel, J.; Karatrantos, A.; Perbal, S.; Senf, B.; Hiekel, A.; Reinhardt, H.; Rauscher, A.; Mäder, T. Review of State-of-the-art of structural health monitoring in hydrogen composite pressure vessels. *Compos. Part C Open Access* **2025**, *18*, 100635. [CrossRef]
2. Kamineni, J.N.; Burela, R.G. Modeling, fabrication, and burst testing of type-IV 3D printed plastic liner composite overwrapped pressure vessels. *Int. J. Interact. Des. Manuf.* **2025**, *19*, 1025–1034. [CrossRef]
3. Bouhala, L.; Koutsawa, Y.; Karatrantos, A.; Bayreuther, C. Design of Type-IV Composite Pressure Vessel Based on Comparative Analysis of Numerical Methods for Modeling Type-III Vessels. *J. Compos. Sci.* **2024**, *8*, 40. [CrossRef]
4. Bouhala, L.; Karatrantos, A.; Reinhardt, H.; Schramm, N.; Akin, B.; Rauscher, A.; Mauersberger, A.; Taşkıran, S.T.; Ulaşlı, M.E.; Aktaş, E.; et al. Advancement in the Modeling and Design of Composite Pressure Vessels for Hydrogen Storage: A Comprehensive Review. *J. Compos. Sci.* **2024**, *8*, 339. [CrossRef]
5. Meemary, B.; Vasiukov, D.; Deléglise-Lagardère, M.; Chaki, S. Sensors integration for structural health monitoring in composite pressure vessels: A review. *Compos. Struct.* **2025**, *351*, 118546. [CrossRef]
6. Mäder, T.; Senf, B.; Hamm, M.; Zoch, M.; Drossel, W.-G.; de Sosa, I.N.; Wolf, P. Shape memory strain gauges. *Proc. Sens.* **2017**, *31515*, 478–482.
7. Mäder, T.; Heusinger, J.V.; Senf, B.; Zoch, M.; Winkler, A.; Drossel, W.-G. Calibration of piezoresistive shape-memory alloy strain sensors. *J. Intell. Mater. Syst. Struct.* **2022**, *33*, 1465–1472. [CrossRef]
8. Otsuka, K.; Ren, X. Physical metallurgy of Ti–Ni-based shape memory alloys. *Prog. Mater. Sci.* **2005**, *50*, 511–678. [CrossRef]
9. Duerig, T.W.; Bhattacharya, K. The Influence of the R-Phase on the Superelastic Behavior of NiTi. *Shape Mem. Superelasticity* **2015**, *1*, 153–161. [CrossRef]

Disclaimer/Publisher's Note: The statements, opinions and data contained in all publications are solely those of the individual author(s) and contributor(s) and not of MDPI and/or the editor(s). MDPI and/or the editor(s) disclaim responsibility for any injury to people or property resulting from any ideas, methods, instructions or products referred to in the content.